Quantitative Measurement of the Three-dimensional Structure of the Vocal Folds and Its Application in Identifying the Type of Cricoarytenoid Joint Dislocation

*Xinlin Xu, †Yong Wang, †Jingan Wang, ‡Jacob F. Reiss, *Li Zhou, ‡Jack J. Jiang, and *Peiyun Zhuang, *†*Xiamen, China, and* ‡*Madison, Wisconsin*

Summary: Objective. The objective of this study was to quantitatively measure the three-dimensional (3D) structure of the vocal folds in normal subjects and in patients with different types of cricoarytenoid dislocation. We will analyze differences in parameters between the groups and also determine if any morphologic parameters possess utility in distinguishing the type and the degree of cricoarytenoid dislocation.

Study Design. This retrospective study was conducted using university hospital data.

Methods. Subjects' larynges were scanned using dual-source computed tomography (CT). The normal subjects were divided into deep-inhalation and phonation groups, and patients with cricoarytenoid joint dislocation were divided into anterior-dislocation and posterior-dislocation groups. Membranous vocal fold length and width were measured directly on the thin-section CT images. Vocal fold and airway 3D models were constructed using *Mimics* software and used in combination to measure vocal fold thickness, subglottal convergence angle, and oblique angle of the vocal folds.

Results. The phonation group displayed a greater vocal fold width, greater oblique angle, thinner vocal folds, and a smaller subglottal convergence angle than those of the deep-inhalation group ($P < 0.05$). The anterior-dislocation group displayed a smaller oblique angle and subglottal convergence angle than the posterior-dislocation group ($P < 0.05$).

Conclusions. The 3D structure of the vocal folds during deep inhalation and phonation can be accurately measured using dual-source CT and laryngeal 3D reconstruction. As the anterior-dislocation group yielded negative values for the oblique angle and the posterior-dislocation group yielded positive values, the oblique angle of the vocal folds may possess utility for distinguishing the type and for quantitatively determining the degree of cricoarytenoid dislocation.

Key Words: Vocal fold−3D model−Morphologic structure−Subglottal convergence angle−Cricoarytenoid joint dislocation.

INTRODUCTION

The morphologic parameters of the vocal folds, such as incomplete glottal closure, glottal area, vocal fold length, vocal fold width, and supraglottal compression, play crucial roles in voice function.[1−3] In recent years, the vocal folds are increasingly being recognized as a three-dimensional (3D) structure that vibrates to form a mucosal wave motion during phonation.[4]

During phonation, the contraction of intrinsic laryngeal muscles and the motion of the arytenoid cartilage may lead to 3D morphologic changes in the vocal folds. The motion of the arytenoid cartilage is a 3D planar motion, where it slides medially, superiorly, and posteriorly on the cricoid cartilage during phonation.[5] The contraction of the thyroarytenoid and the cricothyroid muscles during phonation may lead to changes in vocal fold thickness, which, in turn, may alter the 3D structure of the vocal folds.[6]

Cricoarytenoid joint dislocation refers to the dislocation of arytenoid cartilage in the cricoarytenoid joint capsule. Its clinical manifestations include hoarseness and apparent breathiness.[7] It is evident with laryngoscopy that the ipsilateral vocal folds of patients with cricoarytenoid joint dislocation are fixed to one side. Based on the relationship between cricoid and arytenoid cartilages, as well as on characteristics such as the movement of cuneiform cartilages and the positioning of the vocal folds on the vertical plane, the direction of the dislocation may be preliminarily and qualitatively divided into anteromedial dislocation and posterolateral dislocation. Further diagnosis with laryngeal electromyography (LEMG) and 3D reconstruction of laryngeal computed tomography (CT) allows cricoarytenoid dislocation to be further classified, based on the degree of dislocation, into complete dislocation and subluxation.[8,9] Current clinical studies that quantitatively assess the type and the degree of dislocation, as well as the method of assessment, are relatively rare.

Treatment for patients with cricoarytenoid joint dislocation is usually done by closed reduction based on the type of dislocation. Because of the small size and the location of the cricoarytenoid joint in the larynx, reverse reduction of different intensities is mainly selected for these patients according to the direction and the degree of dislocation. Therefore, the diagnosis and the quantitative determination of the cricoarytenoid joint dislocation direction may bear clinical significance.

The present study aimed to quantitatively measure the 3D structure of the vocal folds and to explore its role in identifying patients with cricoarytenoid joint dislocation. To perform this, membranous vocal fold length and width were measured using

Accepted for publication February 28, 2018.

Disclosure: This study was supported by the National Natural Science Foundation of China, item number 81371080.

From the *Division of Otolaryngology, Xiamen University Zhongshan Hospital, Xiamen, Fujian, China; †Radiology Department, Xiamen University Zhongshan Hospital, Xiamen, Fujian, China; and the ‡Department of Surgery, Division of Otolaryngology−Head and Neck Surgery, University of Wisconsin−Madison School of Medicine and Public Health, Madison, Wisconsin.

Address correspondence and reprint requests to Peiyun Zhuang, Xiamen University Zhongshan Hospital, Division of Otolaryngology, 201-209 Hubin South Road, Xiamen, Fujian, 361004, China. E-mail: peiyun_zhuang@yahoo.com

Journal of Voice, Vol. 33, No. 5, pp. 611−619

0892-1997

https://doi.org/10.1016/j.jvoice.2018.02.024

laryngeal CT, and vocal fold and airway 3D models were reconstructed using *Mimics* software which is from Materialise in Belgium to measure vocal fold thickness, subglottal convergence angle, and oblique angle of the vocal folds. For normal subjects, these metrics were analyzed during both deep inhalation and phonation to investigate the morphologic patterns of the vocal folds during the different tasks. These results will also be used to evaluate the nondislocated side of the vocal folds in patients with cricoarytenoid joint dislocation. For subjects with cricoarytenoid joint dislocation, these metrics were analyzed only during deep inhalation to determine if certain metrics are indicative of the type and the degree of cricoarytenoid joint dislocation in patients.

TABLE 1.
Information of Normal Subjects

Subject	Gender	Age (y)
1	Male	60
2	Female	48
3	Male	54
4	Female	32
5	Female	39
6	Male	58
7	Female	47
8	Male	52
9	Female	34
10	Male	40

TEST SUBJECTS

All subjects volunteered to participate in the present study and signed an informed consent form.

A total of 10 normal subjects (5 men and 5 women), with a mean age and standard deviation of 46.4 ± 9.82 years, were recruited. These subjects did not have voice disorders and agreed to undergo strobolaryngoscopy, which confirmed that the subjects had smooth bilateral vocal fold edges with normal motions and closures while pronouncing /i/. Enhanced neck scanning where the subjects' necks were scanned three times because of other reasons was utilized so that both deep inhalation and phonation could be measured and analyzed.

A total of 10 patients with cricoarytenoid joint dislocation (5 men and 5 women), with a mean age and standard deviation of 46.4 ± 10.5 years, were recruited. Among these patients, five were diagnosed with anterior dislocation and five were diagnosed with posterior dislocation. The patients with cricoarytenoid joint dislocation included in the study were diagnosed using strobolaryngoscopy, LEMG, and laryngeal 3D reconstruction,[8,10] and can be diagnosed specifically as having posterior or arytenoid dislocation (Tables 1 and 2).

Strobolaryngoscopy: Compressive stress during phonation, hemorrhage on the surface of the cuneiform cartilage, and a slight prominence on the medial wall of the piriform fossa were observed in patients with cricoarytenoid joint dislocation. The inferior and the superior shifts of the laterofixed vocal folds and vocal process on the vertical plane indicate anterior and posterior dislocations, respectively (Figure 1).

LEMG examination: All patients with cricoarytenoid joint dislocation underwent thyroarytenoid muscle, cricothyroid muscle, and posterior cricoarytenoid muscle examinations to rule out the possibility of nerve palsy (see Table 3 for the time limit and the amplitude). There were no fibrillation potentials or positive sharp waves in the LEMG examinations, which confirms mechanical injury in the muscles rather than paralysis.

Laryngeal CT scan or 3D reconstruction: All patients with cricoarytenoid joint dislocation underwent CT scanning, and the dislocation was diagnosed based on the presence of compressive stress or gap widening in the cricoarytenoid joint. The type of dislocation was determined based on the location of arytenoid and cricoid cartilages. Arytenoid cartilage located posterior or posterosuperior to the cricoid cartilage indicates a posterior dislocation, whereas arytenoid cartilage located anterior or anteroinferior to the cricoid cartilage indicates an anterior dislocation (Figures 2 and 3).

Laboratory equipment and software

Siemens SOMATOM Definition Flash dual-source CT scanner which is from Siemens in German, *Mimics 10.0* software

TABLE 2.
Information of Patients With Cricoarytenoid Joint Dislocation

	Gender	Age (y)	Hoarse Time (wk)	Direction	Side	Etiology
1	Male	61	4	Posterior	Left	Intubation
2	Female	50	10	Posterior	Left	Intubation
3	Male	53	3	Posterior	Right	Intubation
4	Female	31	6	Posterior	Right	Intubation
5	Female	40	8	Posterior	Right	Intubation
6	Male	60	15	Anterior	Left	Intubation
7	Female	45	8	Anterior	Left	Intubation
8	Male	50	6	Anterior	Left	Intubation
9	Female	32	20	Anterior	Left	Intubation
10	Male	42	12	Anterior	Left	Intubation

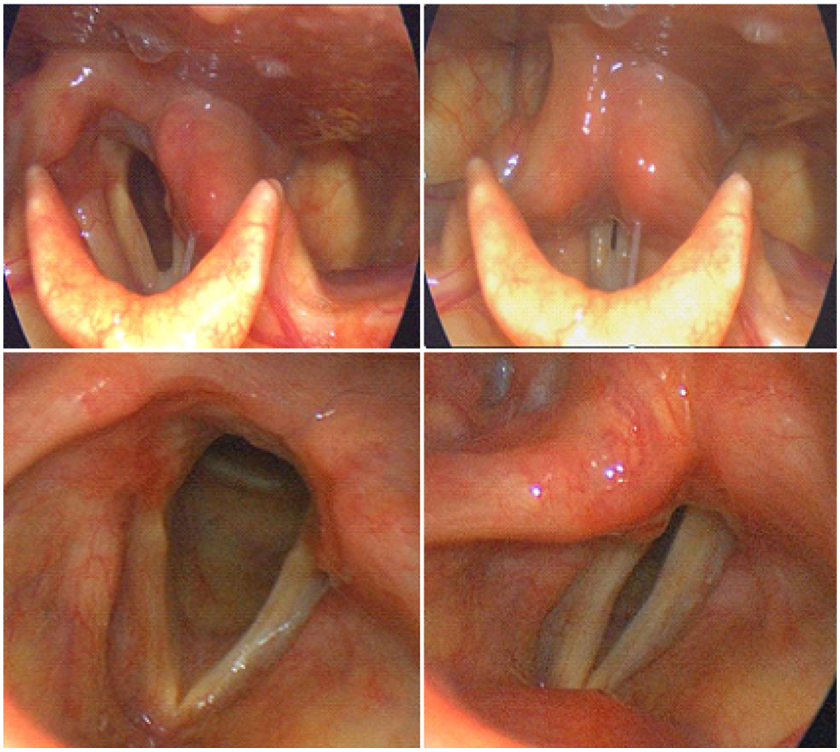

FIGURE 1. Strobolaryngoscopic images of patients with anterior dislocation (*top*) and posterior dislocation (*bottom*) of the left cricoarytenoid joint.

TABLE 3.
Laryngeal Electromyography of Laterofixed Vocal Cords

	Phonation		Deep Inhalation	
	Time Limit (ms)	Amplitude (μV)	Time Limit (ms)	Amplitude (μV)
Thyroarytenoid muscle	7.04 ± 0.89	222.14 ± 107.42	6.81 ± 0.71	208.14 ± 54.98
Cricothyroid muscle	6.41 ± 0.37	211.50 ± 64.56	6.47 ± 0.52	207.50 ± 72.16
Posterior cricoarytenoid muscle	6.86 ± 0.50	246.93 ± 103.44	6.71 ± 0.46	219.79 ± 94.58

Values reported are means with standard deviations.

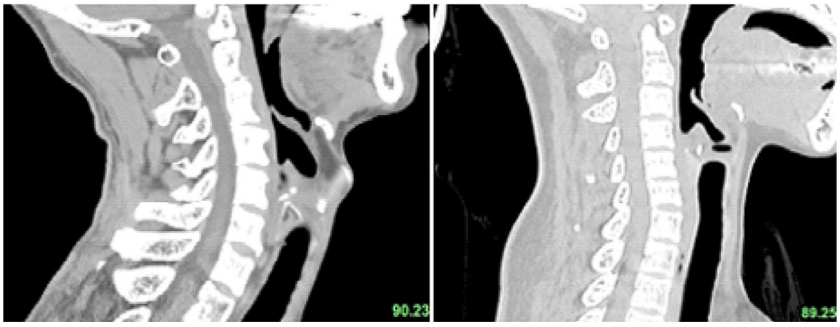

FIGURE 2. Sagittal CT images showing patients with posterior (*left*) and anterior (*right*) cricoarytenoid joint dislocations.

which is from Materialise in Belgium, and *SPSS19.0* which is from IBM in America were used in the study.

Experimental methods

Experimental grouping

(1) Normal subjects who underwent CT scanning while pronouncing /i/ were assigned to the phonation group. Subjects who were scanned while inhaling deeply were assigned to the deep-inhalation group.
(2) Patients with cricoarytenoid joint dislocation who underwent CT scanning during deep inhalation were divided into anterior-dislocation and posterior-dislocation groups based on diagnosis with strobolaryngoscopy and CT 3D reconstruction.

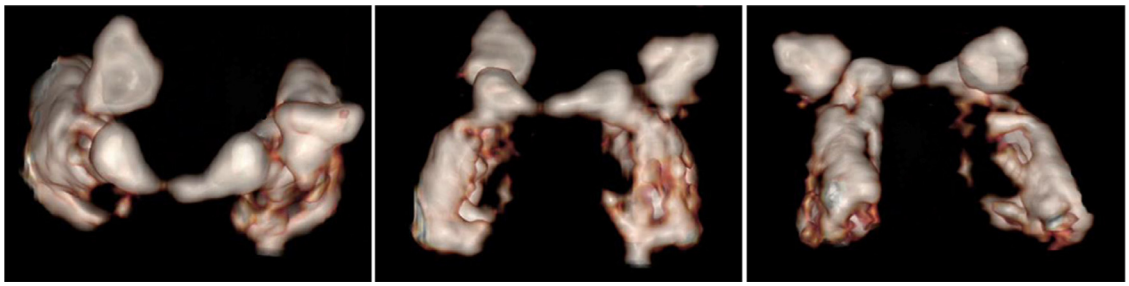

FIGURE 3. The 3D reconstruction images of a patient with anterior dislocation of the left cricoarytenoid joint showing anteromedial dislocation of the left vocal fold.

Definitions of parameters for the 3D structure of the vocal folds

(1) Membranous vocal fold length: This is the distance from the anterior commissure of the vocal folds to the vocal process.
(2) Vocal fold width: This is the vertical distance from the midpoint of the medial edge of the membranous vocal folds to the medial edge of the thyroid cartilage plate.
(3) Subglottal convergence angle: The approximated oblique section of the vocal folds was determined via the lower lip line of the vocal folds and the line between the vocal folds and the tracheal wall. Subglottal convergence angle refers to the intersection angle between the oblique section and the superior edge of the vocal folds at the one-third section of the coronal plane. Please refer to our previous study for more information.[11]
(4) Vocal fold thickness: This is the distance from the transverse line of the superior edge of the vocal folds on the coronal plane of the midpoint of the membranous vocal folds to the lowest point of the inferior edge of the vocal folds.
(5) Oblique angle of the vocal folds: This is the angle between the superomedial edge and the transverse line of the vocal cords.

Measurement of parameters for the 3D structure of the vocal folds

(1) The membranous vocal fold length and width were directly measured with CT (see Figure 4).
(2) The subglottal convergence angle was measured by reconstructing and combining the vocal fold and airway models using the following protocol.

First, the DICOM images of the CT scan were imported into *Mimics* software. Next, the CT threshold level of air was selected to generate the airway model using the coordinate box that included the airway. In the airway model, intersections between the lower lip line and the lateral edge of the vocal folds with the tracheal wall were confirmed to determine the oblique section of the vocal folds. Finally, the CT threshold level of air was reselected to generate the vocal fold model using the coordinate box from the anterior commissure of the vocal folds to the midpoint of the membranous vocal folds. The position of the coronal plane for the measurement of the oblique angle could be determined by the midpoint of the membranous vocal folds, whereas the transverse plane for the measurement of the oblique section of the vocal folds could be determined by the position of the transverse plane on the model.

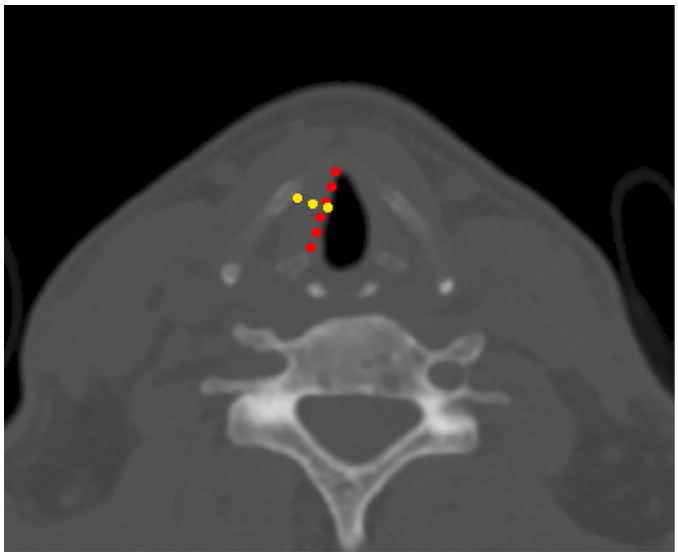

FIGURE 4. Measurement of the membranous vocal fold length (*red*) and width (*yellow*). (For interpretation of the references to color in this figure legend, the reader is referred to the Web version of this article.)

Once the airway and the vocal fold models were combined using *Mimics* software, the subglottal convergence angle was measured by determining the midpoint of the vocal folds using angle measurement tools (Figure 5). Please refer to our previous study for additional information on the measurement of the subglottal convergence angle.[11]

(3) Vocal fold thickness was measured by reconstructing and combining the airway and the vocal fold models using the following protocol.

First, the DICOM images of the CT scan were imported into *Mimics* software. Next, the CT threshold level of air was selected to generate the airway model using the coordinate box that included the airway. In the airway model, the intersection between the most inferior part of the vocal folds and the tracheal wall was confirmed to determine the inferior edge of the vocal folds, whereas the inferior transverse plane for the

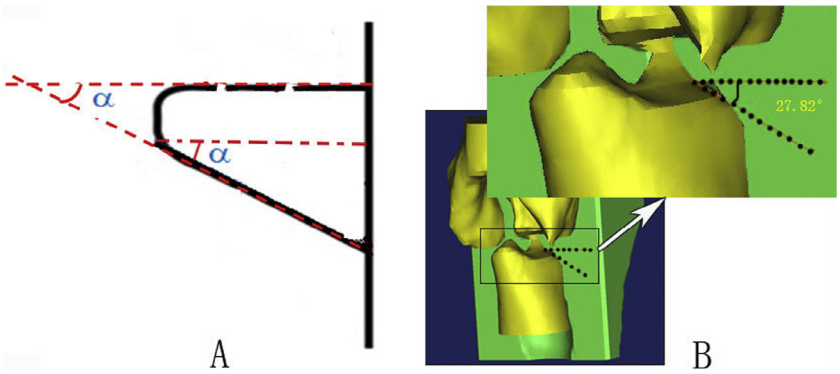

FIGURE 5. Diagram showing the measurement of the subglottal convergence angle (*arrow*). **A.** Schematic diagram. **B.** The combination of airway and vocal fold models for the quantitative measurement.

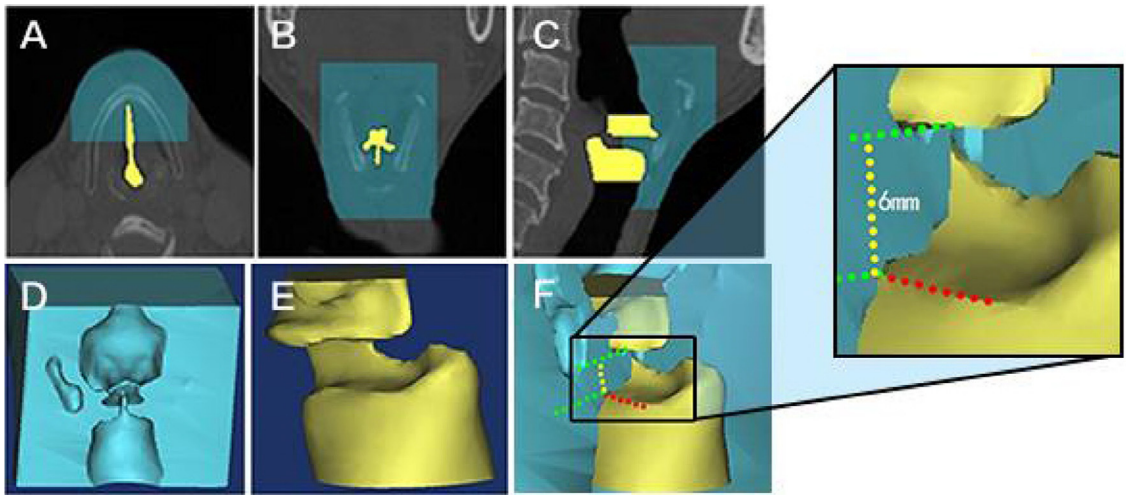

FIGURE 6. Diagrams showing the measurement of vocal fold thickness via the combination of airway and vocal fold models. **A.–C.** Selection of the coordinate box that includes the airway (*yellow*) and the vocal fold (*blue*). **D.** The model of the vocal fold. **E.** The model of the airway. **F.** The combination of airway and vocal fold models for the quantitative measurement of vocal fold thickness. The red dots are for inferior edge of vocal fold. The green dots are for inferior and superior transverse line of vocal fold. The yellow dots are for the measurement of vocal fold thickness. (For interpretation of the references to color in this figure legend, the reader is referred to the Web version of this article.)

measurement of vocal fold thickness was determined by the transverse plane of the intersection. Next, the CT threshold level of air was reselected to generate the vocal fold model using the coordinate box from the anterior commissure of the vocal folds to the midpoint of the membranous vocal folds. The position of the coronal plane for the measurement of vocal fold thickness was determined by the midpoint of the membranous vocal folds, whereas the superior transverse plane for the measurement of vocal fold thickness was determined by the transverse line of the superior edge of the vocal folds.

The airway and the vocal fold models were combined using *Mimics* software for the measurement of vocal fold thickness (Figure 6).

(4) The oblique angle of the vocal folds was measured by reconstructing the vocal fold model using the following protocol.

First, the DICOM images of the CT scan were imported into *Mimics* software. Next, the CT threshold level of the soft tissue was selected for the generation of the vocal fold model using the coordinate box that included the unilateral vocal fold. The line from the midpoint of the membranous vocal folds to the anterior commissure of the vocal folds and the transverse line of the anterior commissure of the vocal folds to the vertex point of the anterior commissure were used in combination to measure the oblique angle of the vocal folds (the angle determined by a vertex and two lines). The angle measured when the vocal folds tilted inferiorly was taken as a negative angle (Figure 7).

Statistical analyses

The statistical analyses were conducted using *SPSS* software. The mean and the standard deviation for the membranous vocal fold length, width, thickness, subglottal convergence angle, and oblique angle of the vocal folds were calculated for normal subjects, as well as for the dislocated cricoarytenoid joint and the nondislocated cricoarytenoid joint. The deep-inhalation and phonation groups were compared using paired *t* tests. Differences in parameters between the

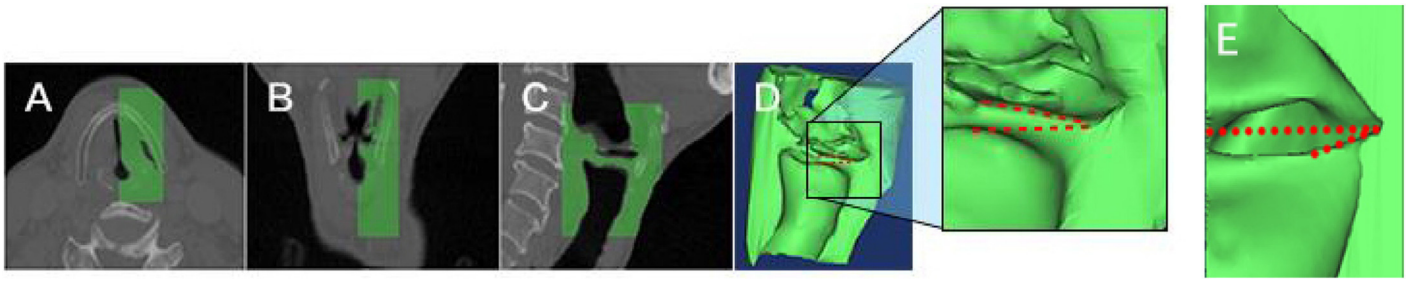

FIGURE 7. Diagrams showing the reconstructed vocal fold model and the measurement of the oblique angle of the vocal folds. **A.–C.** Selection of the coordinate box that includes the vocal fold (*green*). **D.** Vocal fold model for the quantitative measurement of the oblique angle (**D** is for posterior arytenoid dislocation, red dots stand for two lines, the line from the midpoint of the membranous vocal folds to the anterior commissure of the vocal folds and the transverse line. These two lines were used to measure the oblique angle, **E** is for anterior arytenoid dislocation, the meaning of red dots is the same of **D**). (For interpretation of the references to color in this figure legend, the reader is referred to the Web version of this article.)

TABLE 4.
Comparison of Parameters for the Three-dimensional Structure of the Vocal Folds in Normal Subjects During Deep Inhalation and Phonation ($P < 0.05$ Is Significant)

Group	Length (mm)	Width (mm)	Thickness (mm)	Subglottal Convergence Angle (Degree)	Oblique angle of Vocal Folds (Degree)
Deep-inhalation group	12.68 ± 1.85	6.35 ± 0.78	9.47 ± 0.97	74.12 ± 6.67	10.76 ± 9.02
Phonation group	14.93 ± 4.41	8.03 ± 1.03	6.27 ± 1.68	34.95 ± 6.46	19.81 ± 5.84
T value	1.486	3.874	5.224	13.338	2.661
P value	0.155	0.001	0.000	0.000	0.016

anterior-dislocation and the posterior-dislocation groups were analyzed using an independent sample *t* test. Differences in parameters between the nondislocated and the dislocated edges of the vocal folds for the anterior-dislocation and the posterior-dislocation groups were compared using a paired *t* test.

Experimental results

(1) The membranous vocal fold length, width, thickness, subglottal convergence angle, and oblique angle of the vocal folds could be quantitatively measured.
(2) Comparison of parameters for the 3D structure of the normal vocal folds: The mean and the standard deviation of each parameter for the normal vocal folds during phonation and deep inhalation are shown in Table 4.

The membranous vocal folds of the phonation group were longer than those of the deep-inhalation group, but the difference was not statistically significant ($P > 0.05$); the vocal fold width and the oblique angle of the phonation group were significantly greater than those of the deep-inhalation group ($P < 0.05$). The vocal fold thickness and the subglottal convergence angle of the phonation group were significantly less than those of the deep-inhalation group ($P < 0.05$).

(3) Comparison of parameters for the 3D structure of the vocal folds in different types of cricoarytenoid joint dislocation: The mean and the standard deviation of each parameter for the anterior-dislocated and the posterior-dislocated groups during deep inhalation are shown in Table 5. Both the subglottal convergence angle and the oblique angle of the dislocated vocal fold edge in the anterior-dislocation group were significantly smaller than those of the posterior-dislocation group ($P < 0.05$). However, there was no significant difference between the two dislocation groups with respect to vocal fold length, width, and thickness ($P > 0.05$). There was no significant difference between the anterior-dislocation and posterior-dislocation groups with respect to each parameter for the nondislocated side of the vocal folds ($P > 0.05$).

The mean and the standard deviation of each parameter for the comparison between the cricoarytenoid joint-dislocated and nondislocated sides of the vocal folds are shown in Table 6. The dislocated side of the anterior-dislocation group had significantly shorter, wider, and thinner membranous vocal folds than the nondislocated side ($P < 0.05$), but the vocal folds were not longer. The dislocated side had a significantly smaller subglottal convergence angle and oblique angle than the nondislocated side ($P < 0.05$). The structure of the vocal folds with posterior dislocation showed similar alterations, but there was no significant difference for any of the metrics ($P > 0.05$).

Receiver operating characteristic analysis using the oblique angle of the anterior-dislocated vocal fold (n = 5) vs the posterior-dislocated vocal fold (n = 5) yielded an area under the curve value of 1 (Figure 8).

TABLE 5.
Comparison of Parameters for the Three-dimensional Structure of the Vocal Folds in Different Types of Cricoarytenoid Joint Dislocation ($P < 0.05$ Is Significant)

	Comparison of the Cricoarytenoid Joint-dislocated Side of Vocal Folds					Comparison of Nondislocated Vocal Fold Side in Patients With Cricoarytenoid Joint Dislocation				
Group	Length (mm)	Width (mm)	Thickness (mm)	Subglottal Convergence Angle (Degree)	Oblique Angle of Vocal Folds (Degree)	Length (mm)	Width (mm)	Thickness (mm)	Subglottal Convergence Angle (Degree)	Oblique Angle of Vocal Folds (Degree)
Anterior-dislocation group	15.08 ± 2.97	7.20 ± 1.17	5.65 ± 1.59	48.79 ± 6.25	−9.09 ± 4.45	15.99 ± 2.34	5.04 ± 2.40	7.36 ± 1.01	71.72 ± 4.54	6.82 ± 5.28
Posterior-dislocation group	12.78 ± 1.32	5.75 ± 1.09	5.97 ± 2.05	60.21 ± 3.06	18.79 ± 10.31	12.95 ± 1.36	4.58 ± 0.56	6.02 ± 1.41	77.43 ± 8.61	13.65 ± 4.61
Statistical value *T*	1.43	1.887	0.267	3.317	5.511	2.29	0.366	1.679	1.289	2.033
P	0.197	0.101	0.798	0.013	0.001	0.056	0.725	0.137	0.238	0.082

(4) There was no significant difference between the 3D structure of the nondislocated vocal fold side of the anterior-dislocation and the posterior-dislocation groups and the deep-inhalation group of normal subjects ($P > 0.05$).

DISCUSSION

Several studies have investigated how the morphology of the vocal folds may play important roles in phonation and mucosal wave propagation via vocal fold vibration. Hollien showed that laryngeal size, vocal fold length, and vocal fold thickness change alongside the phonational frequency.[12] Xu et al found that different degrees of incomplete glottal closure resulted in varying subglottal convergence angles and suggested that the subglottal convergence angle affects the stress distribution of subglottal pressure in the oblique section direction, which may, in turn, significantly affect vocal fold vibration.[11] These changes in the direction of stress on the vocal folds will cause vocal fold deformation in that direction, which may further complicate vocal fold oscillation and mucosal wave generation. Studies related to the morphologic structure of normal vocal folds during phonation and deep inhalation may serve as a reference for studying the pathologic structure of the vocal folds, thereby exhibiting a certain clinical value for studies related to the morphology of the vocal folds.

Cricoarytenoid joint dislocation, first reported by Korman in 1973,[13] is one such pathology that may be treated more effectively with an improved understanding of vocal fold morphology in normal and pathologic patients. Norris and Schweinfurth reviewed the incidence, diagnosis, laryngoscopic findings, and treatment of cricoarytenoid joint dislocation, and currently a comprehensive diagnosis involving laryngoscopy, CT, strobolaryngoscopy, and electromyography is recommended to evaluate cricoarytenoid joint dislocation.[14] Laryngoscopy and CT have a diagnostic value in their ability to identify the type of dislocation, but the degree of dislocation may only be qualitatively divided into complete dislocation and subluxation based on the cricothyroid space, and there is still a lack of quantitative studies assessing the degree of dislocation. Because 3D reconstruction yields quantitative values for the morphologic parameters, the results such as differentiation between anterior and posterior dislocation from this study may prove to be useful in progressing toward objective diagnoses for the degree and direction of dislocation.

In the present study, the superomedial sliding of arytenoid cartilage on the cricoid cartilage[5,6] and vocal process adduction during phonation widened the vocal folds, whereas the vocal process shifted superiorly, causing the vocal folds to tilt anteriorly in the sagittal direction. Moreover, the cricothyroid muscle contracted, whereas the thyroid cartilage tilted anteriorly during phonation. These factors caused the vocal folds to tilt at an oblique angle with the transverse plane in the sagittal direction, creating the oblique angle of the vocal folds measured in the present study. Our experimental results show that the oblique angle of the vocal folds during phonation was significantly greater than that during respiration, which confirms some of the previously documented findings on arytenoid cartilage

TABLE 6.
Comparison of Parameters for the Three-dimensional Structure Between the Dislocated and Nondislocated Sides of the Vocal Folds in Different Types of Cricoarytenoid Joint Dislocation ($P < 0.05$ Is Significant)

Comparison Between the Cricoarytenoid Joint-dislocated and Nondislocated Sides of Vocal Folds						
Group	Statistical Value	Length (mm)	Width (mm)	Thickness (mm)	Subglottal Convergence Angle (Degree)	Oblique Angle of Vocal Folds (Degree)
Anterior-dislocation group	*T*	2.79	3.39	5.32	6.75	10.06
	P	0.05	0.03	0.01	0.00	0.00
Posterior-dislocation group	*T*	0.61	2.33	0.10	3.05	1.68
	P	0.58	0.10	0.93	0.06	0.19

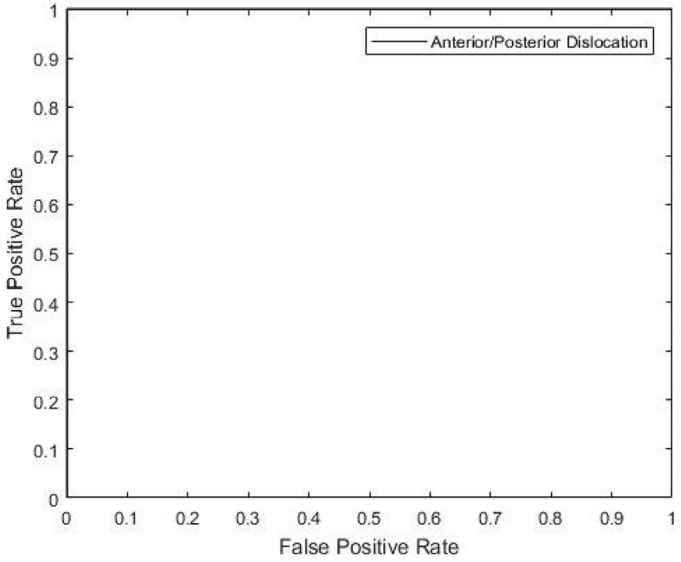

FIGURE 8. Receiver operating characteristic analysis using the oblique angle of the anterior-dislocated vocal fold (n = 5) vs posterior-dislocated vocal fold (n = 5). The line is horizontal at 1, indicating a perfect correlation.

motions.[15,16] Additionally, receiver operating characteristic analysis using the oblique angle of the anterior-dislocated vocal fold (n = 5) vs the posterior-dislocated vocal fold (n = 5) yielded an area under the curve value of 1, meaning that using 3D reconstruction to measure the oblique angle of the vocal fold can perfectly discriminate between an anterior-dislocated or a posterior-dislocated vocal fold. However, the sample size is relatively small for this analysis. According to the principle of material mechanics oblique section stress analysis,[17] the oblique angle of the vocal folds may also alter the direction of the vocal fold mucosal wave motion and vocal fold vibration, which requires further experimental validation.

The size of the subglottal convergence angle during glottal closure measured in the present study corroborates the results of our previous study.[11] Our results also show that the vocal folds during phonation are thinner and wider than during deep inhalation, indicating that vocal fold thinning and widening reduce the subglottal convergence angle. The oblique angle of the vocal folds during phonation differed significantly from the oblique angle during respiration, but the trajectory of the vocal process for each task was similar to that in the study by Wang et al on the motion of the cricoarytenoid joint.[14]

The vocal folds and the vocal process of patients with anterior and posterior dislocations shifted inferiorly and superiorly, respectively. Previously, Mau showed that both the vocal process and the nondislocated side of the vocal folds shifted posteroinferiorly during the anterior subluxation of the cricoarytenoid joint, and that the vocal process shifted to a greater extent than the nondislocated side of the vocal folds. The study also showed that quantitative 3D analysis is conducive to assessing the degree of cricoarytenoid joint subluxation.[15]

In subjects with cricoarytenoid joint dislocation, the anterior-dislocated side of the vocal process shifted inferomedially, with an even more prominent structural difference, as well as wider and thinner vocal folds compared with the nondislocated side of the vocal folds. During the posterior dislocation of the cricoarytenoid joint, the vocal process shifted superiorly and posterolaterally with insignificant changes in vocal fold width and thickness, as confirmed by our results. Given these characteristic shifts, these parameters may also help in identifying the type of dislocation.

In the present study, the membranous vocal fold length did not change during deep inhalation and phonation. This finding may be attributable to vocal fold shortening from vocal process adduction during phonation, offsetting the superior shifting of the vocal process, which elongates the vocal folds. Therefore, the membranous vocal fold length would not change significantly.

The models constructed using the DICOM images obtained from the laryngeal CT scan during phonation may be unstable as the period during each oscillation of the vocal fold vibration cycle differed. This could have affected the experimental results, making further experimental validation necessary. It is also a little unfeasible to construct a comprehensive 3D model for arytenoid and cricoid cartilages as the arytenoid cartilage exhibits varying degrees of calcification in the human body.[16,18] Therefore, the 3D reconstruction of the cricoarytenoid joint is a less suitable as a clinical tool to quantitatively measure the degree of cricoarytenoid joint dislocation. However, the 3D reconstruction of vocal fold soft tissue does not involve the calcification of cartilage, and the oblique angle of the vocal folds is easily measurable using this model. Therefore, the oblique angle of the vocal folds may be used for

determining the type and for quantitatively analyzing the degree of cricoarytenoid joint dislocation. Further experimental validation, however, is still required because of the diagnostic difficulty surrounding CA dislocation.

CONCLUSIONS

There were significant differences in the 3D structure of the vocal folds during phonation and deep inhalation. Compared with deep inhalation, the vocal fold thickness and subglottal convergence angle decreased, whereas the vocal fold width and the oblique angle of the vocal folds increased during phonation. Given the significant difference of the oblique angle between the anterior-dislocated and the posterior-dislocated vocal folds, the oblique angle of the vocal folds may be a useful metric in a clinical setting as a parameter for quantitatively determining the degree and for identifying the type of cricoarytenoid joint dislocation.

REFERENCES

1. Patel R, Dailey S, Bless D. Comparison of high-speed digital imaging with stroboscopy for laryngeal imaging of glottal disorders. *Ann Otol Rhinol Laryngol*. 2008;117:413–424.
2. Khoddami SM, Nakhostin AN, Izadi F, et al. The assessment methods of laryngeal muscle activity in muscle tension dysphonia: a review. *Sci World J*. 2013;2013:77–87.
3. Poburka BJ. A new stroboscopy rating form. *J Voice*. 1999;13:403–413.
4. Krausert CR, Olszewski AE, Taylor LN, et al. Mucosal wave measurement and visualization techniques. *J Voice*. 2011;25:395–405.
5. Berry DA, Montequin DW, Chan RW, et al. An investigation of cricoarytenoid joint mechanics using simulated muscle forces. *J Voice*. 2003;17:47–62.
6. Deguchi S, Kawahara Y, Takahashi S. Cooperative regulation of vocal fold morphology and stress by the cricothyroid and thyroarytenoid muscles. *J Voice*. 2011;25:e255–e263.
7. Saigusa H, Kokawa T, Aino I, et al. Arytenoid dislocation: a new diagnostic and treatment approach. *J Nippon Med Sch Nippon Ika Daigaku zasshi*. 2003;70:382.
8. Rubin AD, Hawkshaw MJ, Moyer CA, et al. Arytenoid cartilage dislocation: a 20-year experience. *J Voice*. 2006;19:687–701.
9. Zhuang P, Nemcek S, Surender K, et al. Differentiating arytenoid dislocation and recurrent laryngeal nerve paralysis by arytenoid movement in laryngoscopic video. *Otolaryngol Head Neck Surg*. 2013;149:451.
10. Thayer SR, David BI, Spiegel JR. Arytenoid dislocation: diagnosis and treatment. *Laryngoscope*. 1994;104:1353–1361.
11. Xu X, Wang J, Devine EE, et al. The potential role of subglottal convergence angle and measurement. *J Voice*. 2017;31 116–e1.
12. Hollien H. Vocal fold dynamics for frequency change. *J Voice*. 2014;28:395–405.
13. Komorn RM, Smith CP, Erwin JR. Acute laryngeal injury with short-term endotracheal anesthesia.[J]. *Laryngoscope*. 1973;83:683–690.
14. Norris BK, Schweinfurth JM. Arytenoid dislocation: an analysis of the contemporary literature. *Laryngoscope*. 2011;121:142–146.
15. Wang Q, Liang L, Liu Y, et al. Quantitative analysis of the visor-like vertical motion of the cricoarytenoid joint in the living subject. *J Voice*. 2016;30:354.
16. Mau T. Three-dimensional morphometric analysis of cricoarytenoid subluxation. *J Voice*. 2012;26:133–136.
17. Boresi AP, Chong KP, Lee JD. *Elasticity in Engineering Mechanics*. 3rd ed Hoboken: Wiley; 2010:65.
18. Sataloff RT. *Voice Science*. San Diego: Plural Publishing, Inc.; 2005:178–180.